GENETICS

The Ptch/SPOUT1 methyltransferase deposits an m^3U modification on 28*S* rRNA for normal ribosomal function in flies and humans

Jie Chen[1,2]†, Yaofu Bai[1]†, Yuantai Huang[3]†, Min Cui[4]†, Yiqing Wang[1], Zhenqi Gu[1], Xiaolong Wu[1], Yubin Li[5], Yikang S. Rong[1]*

The ribosomal RNA (rRNA) is one of the most heavily modified RNA species in nature. Although we have advanced knowledge of the sites, functions, and the enzymology of many of the rRNA modifications from all kingdoms of life, we lack basic understanding of many of those that are not universally present. A single N^3 modified uridine base (m^3U) was identified to be present on the 28*S* rRNA from humans and frogs but absent in bacteria or yeast. Here, we show that the equivalent m^3U is present in *Drosophila* and that the Ptch/CG12128 enzyme and its human homolog SPOUT1 are both necessary and sufficient for carrying out the modification. The Ptch-modified U is at a functional center of the large ribosomal subunit, and, consistently, *ptch*-mutant cells suffer loss of ribosomal functions. SPOUT1, suggested to be the most druggable RNA methyltransferases in humans, represents a unique target where ribosomal functions could be specifically compromised in cancer cells.

INTRODUCTION

Chemical modifications play important roles for the functions of RNA molecules. The RNA component of the ribosome, ribosomal RNA (rRNA), is the most abundant RNA species in cells and is also one of the most abundantly modified in both class and number [for reviews, see (*1*–*4*)]. The most abundant modifications on rRNA are 2′-*O*-methylation of the sugar moiety and pseudo-uridylation of the uridine base. The biological functions of these modifications include regulating RNA stability, facilitating base interactions between subunits or different functional centers of the ribosome, allowing for control of translational efficiency and accuracy [reviewed in (*5*–*10*)]. Many of these modifications are evolutionarily conserved. 2′-*O*-methylation and pseudo-uridylation are implemented by methyltransferases and pseudouridine synthases, respectively. The work of these enzymes is usually directed by small nucleolar RNAs (snoRNAs) that base pair with rRNA at the targeted site [reviewed in (*11*–*13*)]. However, some of the methyltransferases are "stand-alone," e.g., the Pet56 enzyme from bacteria (*14*) and Spb1 from yeast (*15*, *16*).

Methylation of rRNA bases is generally abundant, including m^6A, m^5C, and m^3U. These modifications are carried out by stand-alone methyltransferases that do not rely on snoRNAs [e.g., (*17*, *18*)]. Base methylation serves essential functions for the ribosome. For example, the bacterial enzyme KsgA catalyzes two specific m^6A modifications on 16*S* rRNA, which play an important role in translational accuracy (*19*, *20*). More recently, m^6A modifications on human 28*S* and 18*S* rRNAs, mediated by ZCCHC4 and METTL5, respectively, have been shown to regulate global level and dynamics of translation (*21*–*24*). Similar to both 2′-*O*-methylation and pseudo-uridylation of rRNA, base methylation displays organism-specific class and location, suggesting specialized functions.

Methylation at the N^3 position of uridine (m^3U) is one of the least studied base methylations in nature. The m^3U base has a reduced base-pairing strength with the A base due to the loss of one of the two hydrogen bonds. In *Escherichia coli*, the RsmE enzyme is responsible for the methylation of U1498 on 16*S* rRNA. The loss of this modification results in growth defects with a not well-understood mechanism (*25*–*27*). Two modified U bases have been identified on 25*S* rRNA from the budding yeast, and the enzymes Btm5 and Btm6 were identified as the responsible methyltransferases (*17*). Unfortunately, how these modifications contribute to ribosomal functions is also poorly understood.

In 1990, Maden reported a single N^3 modified U base on human and frog rRNAs, which was further confirmed in later studies (*28*, *29*). The modified base of U4500 of the human 28*S* rRNA, with numbering according to the 3D Ribosomal Modification Maps Database (*30*), is one of the two neighboring and universally conserved U bases at the peptidyl transferase center (PTC), an essential functional center of the large ribosome [reviewed in (*31*)]. That U base at PTC is not modified on bacteria or yeast rRNA, suggesting specialized function of this m^3U in higher organisms.

Here, we identify the enzyme responsible for this modification. By mutational analyses, we showed that the conserved Ptch protein is required for the presence of m^3U at eukaryotic PTCs. In addition, purified Ptch proteins from flies and humans are capable of methylating rRNA substrates in vitro. Furthermore, *Drosophila* cells without an m^3U-modified PTC suffer a growth defect accompanied by reduced protein synthesis, while loss of the enzyme is lethal to human cells. The identification of Ptch, a member of the SPOUT class of methyltransferases, as the m^3U methyltransferase of eukaryotic organisms helps to fill a gap in our understanding of rRNA modifications.

[1]MOE Key Lab of Rare Pediatric Diseases, Hengyang College of Medicine, University of South China, Hengyang, China. [2]Plant Protection Research Institute, Guangdong Academy of Agricultural Sciences, Guangdong Provincial Key Laboratory of High Technology for Plant Protection, Guangzhou, China. [3]State Key Laboratory of Oncology in South China, Collaborative Innovation Center for Cancer Medicine, Sun Yat-sen University, Guangzhou, China. [4]School of Public Health, Hengyang College of Medicine, University of South China, Hengyang, China. [5]The First Affiliated Hospital of Jinzhou Medical University, Jinzhou, China.
*Corresponding author. Email: zdqr03@yahoo.com
†These authors contributed equally to this work.

RESULTS

Ptch is a nucleolar protein essential for growth and viability

We conducted a small-scale CRISPR-Cas9–mediated mutagenesis of *Drosophila* genes predicted to encode domains with potential RNA modifying activities [e.g., (*32*)]. For the uncharacterized *CG12128* gene, we recovered frameshift mutations at the C-terminal region that cause recessive phenotypes, which include partial lethality of homozygotes (~75%) and complete female sterility of the survivors, while male homozygous mutants are semi-fertile (fig. S1). The genomic structure of *CG12128* and alleles used in this study are provided in Fig. 1A. 4′,6-Diamidino-2-phenylindole (DAPI) staining of the mutant ovaries revealed that they are filled with egg chambers arrested at early stages of oogenesis (Fig. 1B). On the basis of the morphology of the mutant ovaries, we rename *CG12128* as *pu tao chuan* (*ptch*), which is the Chinese translation of "strings of grapes." In addition to semi-lethality and female sterility, *ptch*-mutant adults display a classic "Minute" phenotype indicative of partial loss of ribosomal functions (*33*, *34*), which includes slow growth, small body sizes, thin and shortened bristles, and sterilities in adults (Fig. 1C and fig. S1B).

We also generated a deletion mutation of *ptch* using two single-guide RNAs (sgRNAs) in CRISPR-Cas9 mutagenesis, deleting the entire methyltransferase domain (Fig. 1A). This mutation, likely null, causes complete lethality at the third instar stage, suggesting that the aforementioned frameshift mutations are likely hypomorphic in nature. All the phenotypes described above—lethality, sterility, and Minute—were rescued with a transgene that carries a genomic fragment of the wild-type *ptch* locus, so was a similar transgene carrying *ptch* but with a C-terminal *egfp* gene fusion (Fig. 1A). In addition, we constructed a transgene in which two Gly

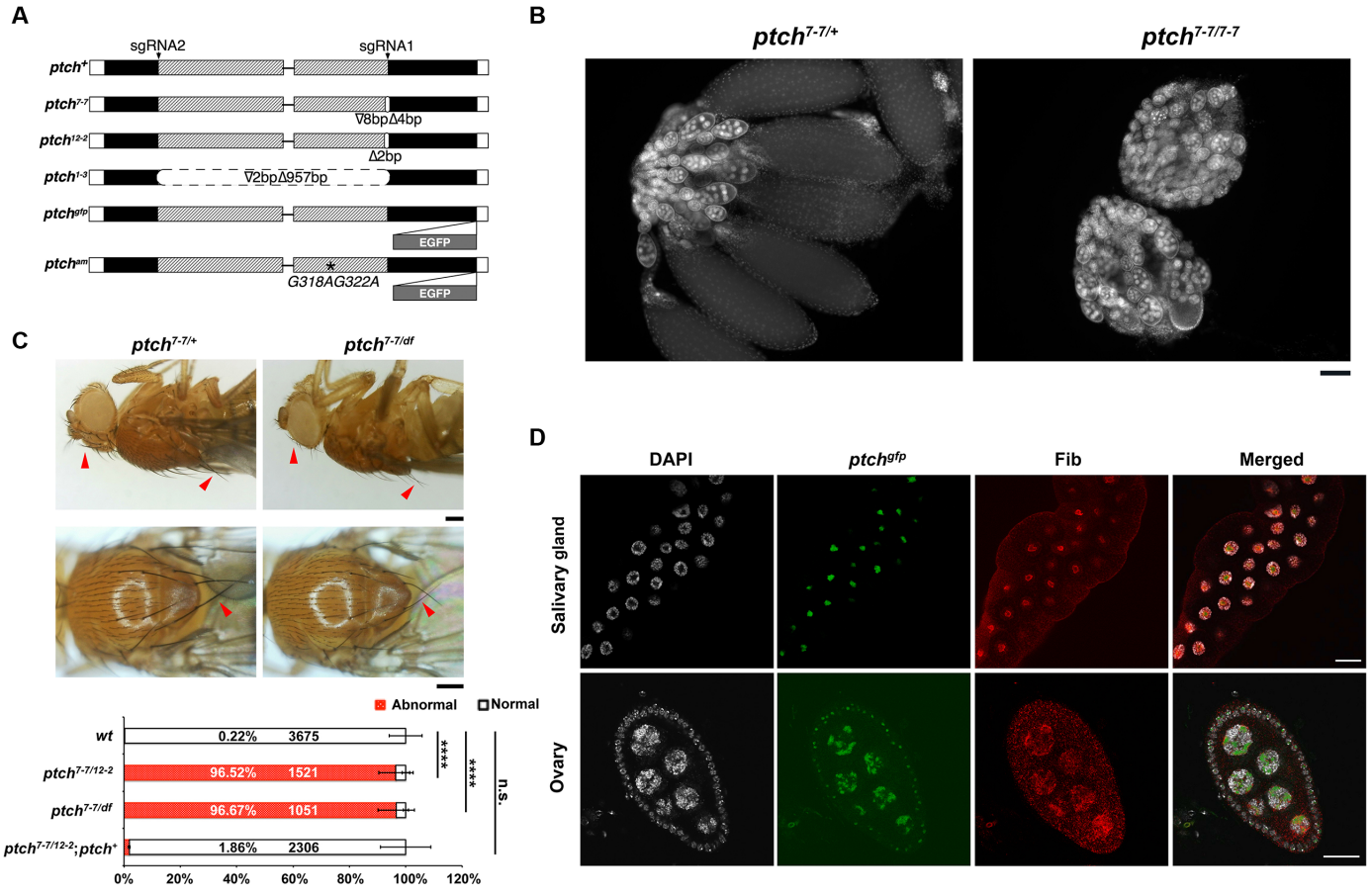

Fig. 1. Ptch is a nucleolar protein essential for animal development. (**A**) Alleles of *ptch*. Rectangular boxes represent exonic regions, and lines indicate introns. Unfilled (white) regions represent UTRs, and filled regions indicate coding regions. The hatched region encodes the methyltransferase domain. The two sgRNA-targeted regions are indicated by arrowheads. The approximate positions of the point mutations are indicated by vertical white bars. In the two transgenic rescuing constructs at the bottom, the EGFP tag and the *G318AG322A* mutation (am) are indicated. Drawings are not to scale. (**B**) Defective oogenesis in *ptch* mutants. 4′,6-Diamidino-2-phenylindole (DAPI) staining of dissected adult ovaries, with genotypes on top, shows normal development in wild-type females in which less mature egg chambers are heavily stained with DAPI, while mature eggs are less stained. In the mutants, only immature egg chambers are present. Scale bar, 100 μm. (**C**) Minute bristles on *ptch* mutants. In the dorsal and the side views of adult flies, the largest bristles on the back and head regions are indicated with red arrowheads, showing the mutants having thinner and shorter bristles. Genotypes are listed on top of the pictures. Quantification of the bristle phenotypes is given below the pictures, with genotypes given to the left. *df*, a chromosomal deficiency of the *ptch* region. ****$P < 0.0001$; n.s., not significant. (**D**) Nucleolar localization of Ptch. Immunostaining of salivary glands from third instar larvae and ovaries from adults, both with the genotype of $ptch^{1\text{-}3/1\text{-}3}$; $[ptch^{gfp/gfp}]$, was performed with an anti-Fib antibody. A single gland or a single-egg chamber is shown with DNA signal in white, $Ptch^{GFP}$ fluorescence signal in green, and anti-Fib signal in red. Merged images of all three signals are also shown. Scale bars, 40 μm. For more Ptch localization images, see fig. S1.

residues predicted to be essential for the methyltransferase activity are mutated to Ala (Ptch^{G318AG322A}, fig. S1 and Fig. 1A). This mutated Ptch protein (Ptch^{am}, active-site mutant), although able to correctly localize (see below and fig. S1), was unable to substitute for the function of the wild-type protein (fig. S1). Together, these results confirm that the mutant phenotypes are due to the loss of Ptch and, primarily, the loss of its methyltransferase function.

To determine the cellular location of Ptch, we first used green fluorescent protein (GFP) fluorescence in tissues of *ptch*^{gfp} animals in which the only class of Ptch proteins are those tagged with enhanced GFP (EGFP; full genotype: *ptch*$^{1\text{-}3/1\text{-}3}$; *ptch*$^{gfp/gfp}$). We discovered that Ptch-GFP are concentrated in the nucleolus. This nucleolar localization was confirmed when Ptch-GFP signals were merged with anti-fibrillarin (Fib) signals in immunostaining experiments, using Fib as a nucleolar marker (Fig. 1D). Ptch also co-localizes with rRNA in the nucleolus in immuno–fluorescence in situ hybridization (FISH) experiments (fig. S1). Therefore, Ptch is a nucleolar protein, likely carrying out molecular functions related to rRNA, which is consistent with the Minute phenotypes described earlier. The Human Ptch homolog, SPOUT1, has been identified as essential for cell viability (*35*, *36*), and overexpressed SPOUT1 protein localizes to the nucleolus (*35*).

The m^{3}U modification of 28*S* rRNA depends on Ptch

The Ptch protein has an annotated methyltransferase domain belonging to the SPOUT family. Members of this family are RNA methyltransferases acting on nucleotide bases on either the rRNA or tRNA (*37*–*40*). The nucleolar localization of Ptch led us to hypothesize that Ptch performs base methylation of rRNA.

A conventional way to detect some of the RNA modifications, particularly 2′-*O*-methylation, is based on reverse transcriptase's reduced ability to traverse a modified base on the RNA template in the presence of restrictive amounts of deoxynucleotide triphosphates (dNTPs). We used the method of "Reverse transcription at low deoxyribonucleoside triphosphate concentrations followed by polymerase chain reaction" [RTL-P; (*41*)] to sample a few regions of the rRNA and identified a small region toward the 3′ end of 28*S* rRNA that yield different reverse transcription polymerase chain reaction (RT-PCR) patterns between the *wt* and *ptch* mutants (fig. S2, A and B). The region that we identified by RTL-P is highly conserved in eukaryotes (fig. S2C). RNA modifications on human 28*S* rRNA have been extensively categorized previously (*29*). We noted that a single N^3 modification of U4500 of the human and U3629 of the frog rRNA was discovered more than 30 years ago (*28*), and the responsible methyltransferase remained unknown.

To investigate whether the corresponding U base (U3485) in fly 28*S* rRNA is modified (Fig. 2A), we used a primer extension method based on the fact that an m^{3}U base partially loses hydrogen-bonding capacity with the A base (Fig. 2B), leading to termination of RT. A similar assay has been used in m^{3}U studies in bacteria and yeast (*17*, *26*). As shown in Fig. 2C, reverse transcription using total RNA from *wt* or *ptch*-heterozygous adults as an RT template produced fragments terminating at the base immediately 3′ to the potentially modified U base, confirming the existence of a modification. The termination was eliminated when *ptch*-homozygous mutant RNA was used in RT, indicating that the modification is abolished by the mutation. A similar primer extension experiment confirmed the presence of the modified U on rRNAs from both the human and mouse but neither budding nor fission yeast rRNAs (Fig. 2D).

To further confirm the presence and map the location of m^{3}U on rRNAs from fly and human, we used a nuclease protection principle to enrich small RNA fragments that either contain or do not contain the modified U base (Fig. 2E) (*42*) and subjected them to either high-performance liquid chromatography (HPLC) or liquid chromatography–tandem mass spectrometry (LC-MS/MS) analyses. As shown in Fig. 2F, HPLC analyses confirmed the presence of m^{3}U in the *wt* RNA fragments that include U3458 but not those without. Similarly, m^{3}U is present in mouse and human but not yeast rRNA, consistent with results from primer extension experiments shown in Fig. 2D. m^{3}U is missing in RNA fragments containing U3458 but isolated from *ptch* mutants (Fig. 2F). As shown in the results from LC-MS/MS analysis (Fig. 2G), m^{3}U signal was present when a 34–nucleotide (nt) oligo protecting the m^{3}U base was used to isolate small rRNA fragments from wild-type RNA (Fig. 2E), whereas m^{3}U was absent when a 30-nt oligo that does not cover the m^{3}U base was used instead (Fig. 2E). In addition, the ratio of m^{3}U over unmodified U bases for the m^{3}U containing fragment is 1/6 (16.67%) in theory, which matches the observed value of 17.36% (Fig. 2G). Therefore, multiple methods were used to confirm the presence of m^{3}U at U3485 of fly 28*S* rRNA and its dependence on Ptch.

To similarly investigate the role of Ptch homolog SPOUT1 in methylating the human rRNA counterpart, we used RNA interference (RNAi) to knock down SPOUT1 expression in HeLa cells. RTL-P, which in wild-type 28*S* rRNA showed impeded reverse transcription because of the m^{3}U modification, was uninterrupted when SPOUT1 expression was reduced (fig. S2C). Therefore, the role of Ptch/SPOUT1 in controlling m^{3}U modification of 28*S* rRNA is evolutionarily conserved.

Loss of m^{3}U at PTC affects translational efficiency

The Ptch-regulated U3485 base is situated in a highly conserved region of PTC of the large ribosomal subunit. The Minute phenotypes carried by *ptch*-mutant adults suggest defective protein synthesis (Fig. 1C). To investigate the efficiency for peptide synthesis in vivo, we used a puromycin-based method. The antibiotic puromycin interacts with the ribosome and gets incorporated into the elongating polypeptide chain, causing its termination. The O-propargyl-puromycin (OPP) derivative of puromycin, engineered with different labels, allows the detection of the newly synthesized polypeptide chains after a click chemistry reaction in both cultured cells and animal tissues (*43*, *44*).

As animals with the *ptch*$^{1\text{-}3}$–null allele die as third instar larvae, we treated larval tissues from both the *wt* and *ptch*$^{1\text{-}3}$ animals with OPP. At different time points after treatment, a click chemistry reaction was performed to label the incorporated OPP with the Alexa Fluor 488 fluorophore. Total proteins were extracted after labeling, and Alexa Fluor 488 fluorophore signals were visualized on a gel, which was subsequently stained for total protein to control for equal loading. As shown in the left panel in Fig. 3A, loss of Ptch reduces the amount of newly synthesized peptide. This suggests that loss of the m^{3}U at PTC impairs peptide synthesis in vivo. However, defective peptide synthesis was not evident when we used the OPP assay on animals mutant for the *ptch*$^{7\text{-}7}$ hypomorphic allele, regardless of whether larval tissues (Fig. 3A, right panels) or dissected testes and ovaries from adults (Fig. 3B) were used for OPP labeling. We suspect that protein synthesis reduction in this partial loss-of-function mutant might not be robust enough for the OPP assay to detect the small decreases in translational efficiency. For example, the synthesis

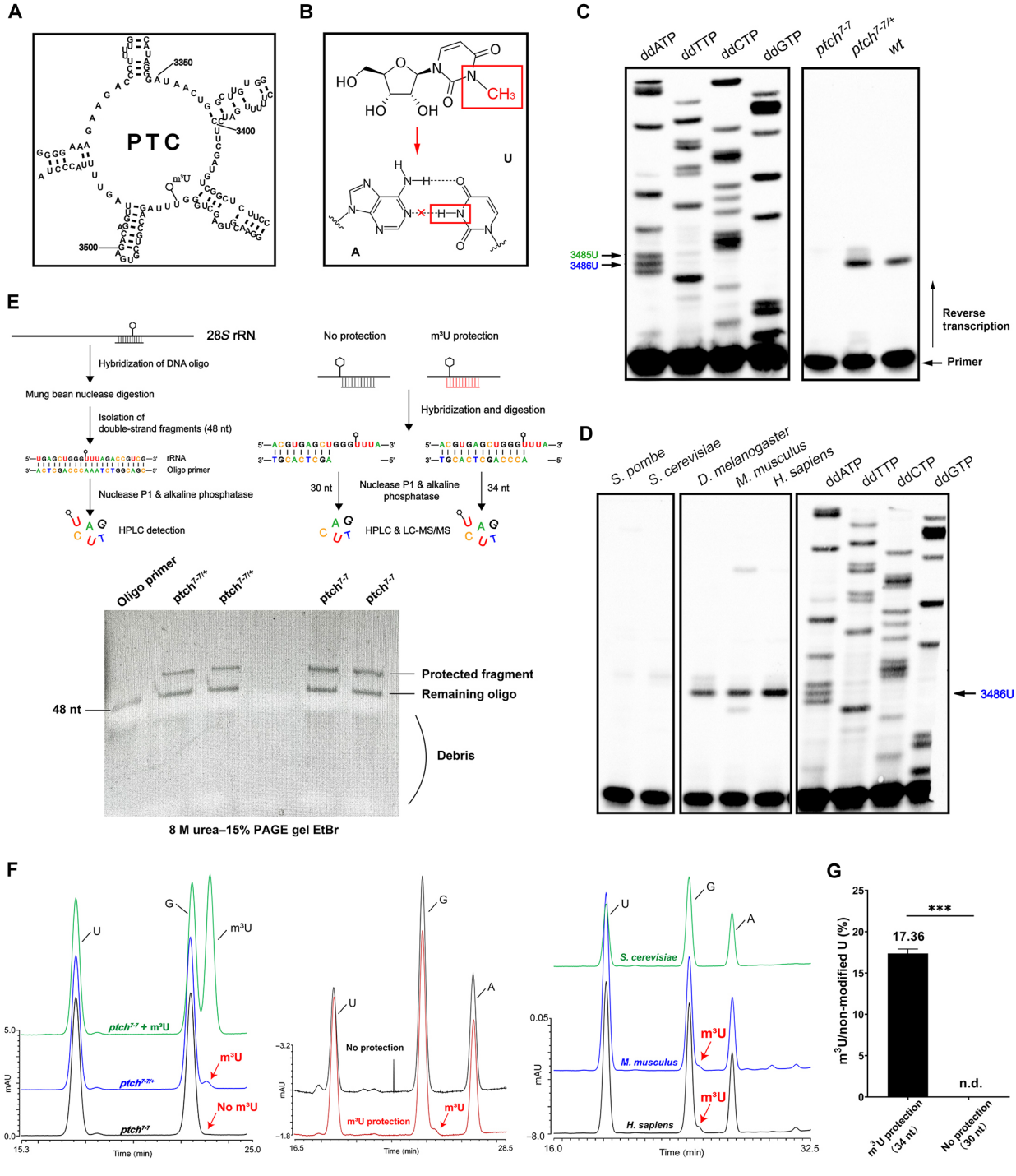

Fig. 2. m^{3}U modification of 28*S* rRNA is controlled by Ptch. (**A**) Schematics of PTC from *Drosophila*. Secondary structure was reproduced from https://rnacentral.org/rna/URS0000A53741/7227. (**B**) The chemical structure of m^{3}U. The methyl group of m^{3}U is outlined in red (top). Hydrogen bonds are shown for a normal A:U pair (bottom). (**C**) Primer extension detection of m^{3}U in *Drosophila* RNA. Results from primer extension are shown to the right with genotypes listed on top. At the left is a sequencing gel, showing the characteristic "triple-U" pattern with U3486 in blue and m^{3}U3485 in green. (**D**) Primer extension detection on eukaryotic rRNAs. The left image shows results from primer extension using total RNA from different organisms. At the right is a sequencing gel. (**E**) Nucleosides isolation by nuclease protection. At the top is a schematic of the procedure, in which DNA primers anneal with rRNA at or near the m^{3}U position (lollipop). Two primers cover the m^{3}U base (situations at the left and the right, "m^{3}U protection"), and one does not (situation in the middle, no protection). At the bottom is an ethidium bromide stained gel showing products after nuclease digestion with genotypes on top. PAGE, polyacrylamide gel electrophoresis. (**F**) RP-HPLC analyses of m^{3}U. At the left, nucleosides were purified from *ptch* heterozygotes (blue line) or homozygotes (green and black lines). A commercial m^{3}U sample was spiked in in the "green" sample. In the middle, nucleosides were purified from wild-type adults with the two primers used in the protection assay as illustrated in (E). At the right, nucleosides were purified from yeast, mouse and human rRNA. (**G**) LC-MS/MS detection of m^{3}U. Nucleosides were purified from *wt* adults, either with a m^{3}U protecting oligo [right situation in (E)] or with one not covering the m^{3}U base [middle situation in (E)], and subjected to MS analyses. n.d., none detected. ***$P < 0.001$.

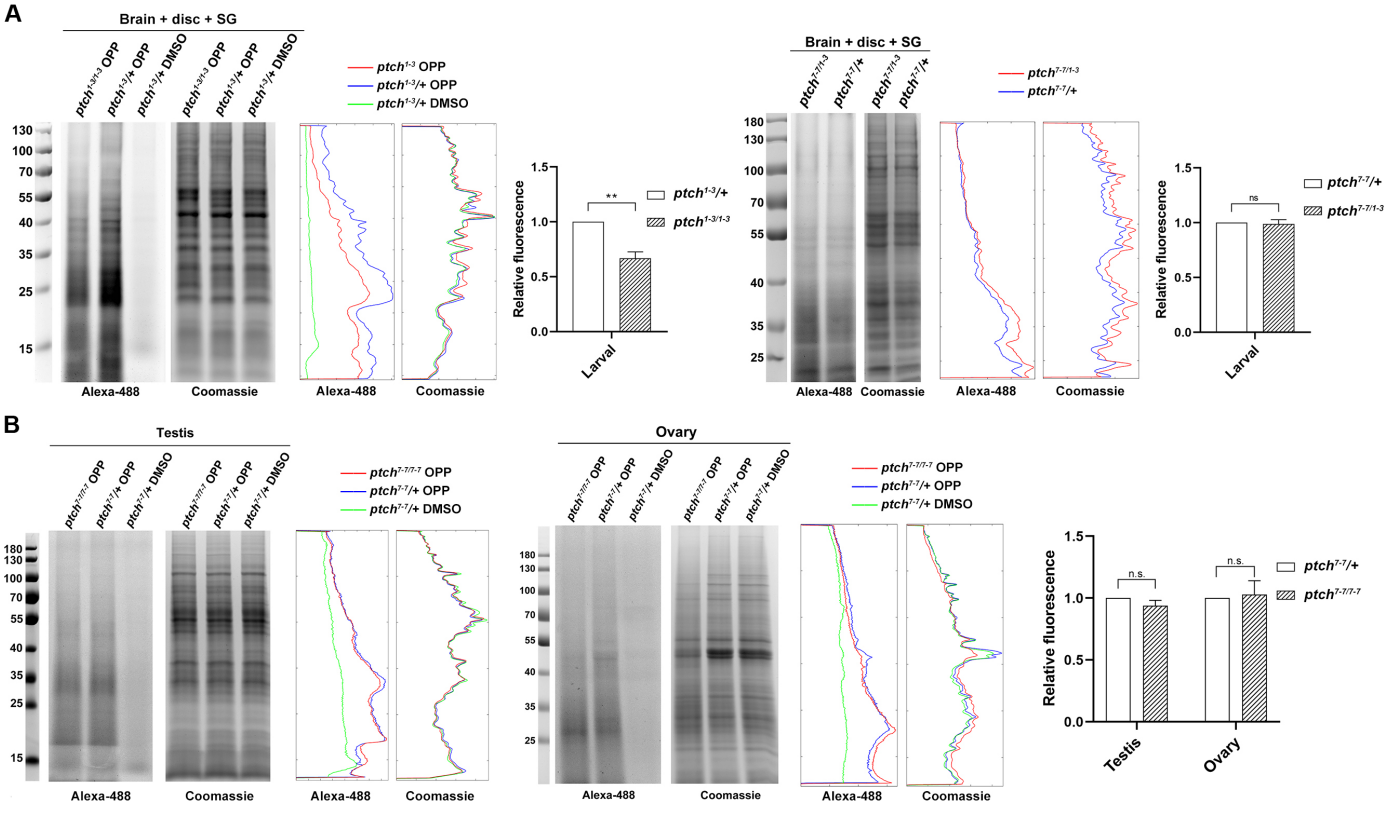

Fig. 3. The effects of Ptch loss on translational efficiency. (**A**) OPP labeling of larval tissues. The tissue samples of salivary glands (SG), imaginal discs, and brains were treated with OPP for 2 hours, followed by a Click-chemistry reaction for attaching the Alexa Fluor 488 fluorophore. Two gel pictures are shown for each experiment: The left panel shows Alexa488-OPP signals, and the right one shows the same gel stained for total protein. Markers with molecular weights in kilodaltons are labeled. Genotypes are shown on top of the gel pictures. A negative control was included in which only the DMSO solvent of OPP was added to account for background fluorescence. Signal quantifications were included for all gel pictures. The chart to the right shows quantification of the OPP signals normalized over the total protein signals. The effects from both the null *ptch*$^{1\text{-}3}$ (left panels) and the hypomorphic *ptch*$^{7\text{-}7/1\text{-}3}$ (right panels) alleles were tested. (**B**) OPP labeling of adult tissues. Testes and ovaries of the indicated genotypes were similarly treated as the larval tissues shown in (A). Alexa488-OPP and total proteins are measured and quantified similarly as in (A). $^{**}P < 0.01$.

of specific classes of proteins rather than total protein synthesis might be disrupted by the hypomorphic mutation.

Mature 5.8*S*, 18*S*, and 28*S* rRNAs are processed from a single pre-rRNA transcript, and the processing follows highly conserved and well-defined steps from yeast to human [fig. S3A; reviewed in (*45*, *46*)]. As Ptch is concentrated at the nucleolus where pre-rRNA processing happens, we investigated whether this processing is abnormal in *ptch* mutants. On overexposed Northern blots using probes from different regions of the rRNA, the amount of rRNA processing intermediates appears normal in the mutant (fig. S3B). In addition, as severe processing defects could reduce the level of mature rRNAs, we used Northern blotting (fig. S3, B and C) and quantitative PCR (qPCR) (fig. S3D) to show that all of the mature species appeared at normal levels in the mutant samples. We therefore conclude that the loss of m^{3}U in 28*S* rRNA does not affect pre-rRNA processing.

The Ptch methyltransferase is sufficient for m^{3}U modification of 28*S* rRNA

To test whether the Ptch enzyme is the sole enzyme responsible for carrying out the N^3 modification, we set out to establish an in vitro methylation assay using purified components. We expressed an maltose-binding protein (MBP)-tagged recombinant Ptch from bacteria and an MBP-Ptch variant that carries single amino acid mutations (Ptch^{G318AG322A} or Ptch^{am}). On the basis of studies of other SPOUT family methyltransferases (*27*, *37*, *39*, *47*–*49*), these mutations would disrupt Ptch's interaction with its cofactor *S*-adenosylmethionine (SAM) and severely impede its methyltransferase activity. The two proteins were thus purified in parallel (fig. S4A) and used in the assay.

As an RNA substrate for the reaction, we used total RNA purified from *wt* or *ptch*$^{7\text{-}7/7\text{-}7}$ mutant adults. The in vitro methylation reaction was followed by primer extension to detect the m^{3}U base. As shown in Fig. 4A, MBP-Ptch, but not MBP-Ptch^{am}, is capable of installing m^{3}U on rRNA of *ptch*-mutant origin at the expected position, and this reaction depends on the presence of SAM. Similarly purified human SPOUT1 recombinant protein was also able to catalyze the specific N^3 modification of *ptch*-mutant rRNA from *Drosophila* (Fig. 4B and fig. S4A), which is indicative of a strong conservation in enzyme substrate recognition. Ptch recombinant protein lacking the MBP tag (fig. S4B) also supports in vitro m^{3}U methylation.

To further investigate how Ptch recognizes its substrate, we used in vitro transcribed fly 28*S* rRNA as substrates. In addition to

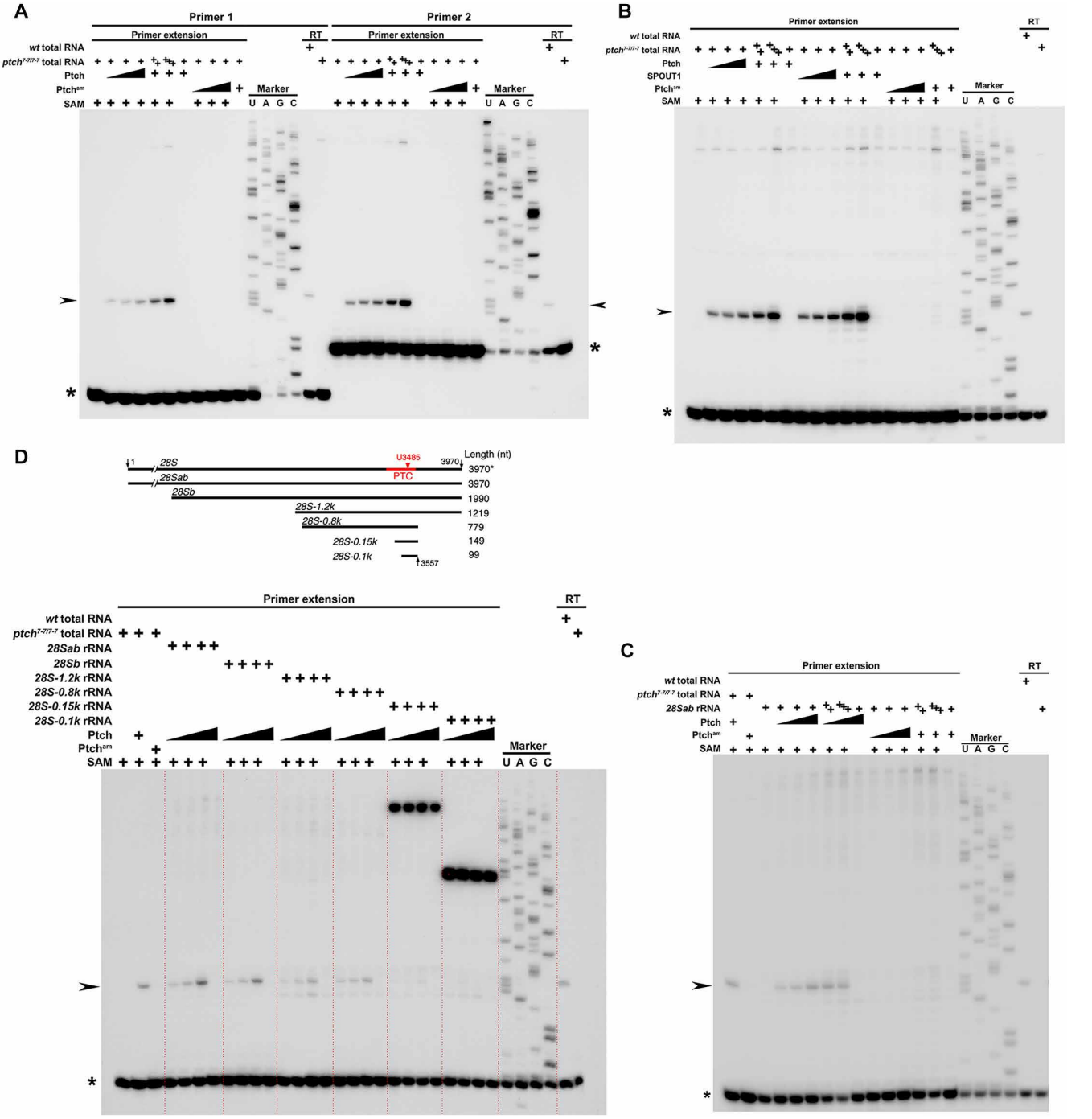

Fig. 4. Ptch is the m^{3}U methyltransferase for 28*S* rRNA. (**A**) In vitro methylation with total RNA. Reaction specifics are listed in Materials and Methods. Total RNA from *ptch* mutants was used in the reaction with recombinant Ptch enzyme or with an active site mutant form of Ptch (Ptch^{am}). The methylation products were subject to primer extension using two different primers, *hyt* ("primer 1") and *2R* ("primer 2"). "UAGC" lanes are DNA sequencing markers. The rightmost two lanes are primer extension results without the preceding methylation reaction. RT, reverse transcription only. Arrowheads mark the stalled product due to the presence of m^{3}U, while free oligos are marked with asterisks. (**B**) SPOUT1 is functional on *Drosophila* substrate. Reaction specifics are listed in Materials and Methods. (**C**) Methylation with in vitro transcribed RNA. Methylation reactions were performed similarly, but with a control reaction using *ptch*-mutant RNA, which was run at the leftmost lane. (**D**) Investigation of substrate specificity. At the top is a schematic representation of the in vitro–transcribed RNA fragments used. Names of the RNA substrates are listed either at the top or to the left of the thick line representing each fragment drawn approximately to scale. The sizes of the fragments are listed to the right. "28*S*" denotes rRNA purified from adults. Although mature 28*S* rRNA is about 3970 nt long, 28*S* purified from flies is often self-cleaved yielding the 28Sb fragment. Key positions are labeled with arrows with the nucleotide numbers given. The position of the PTC is shown in red with m^{3}U3485 labeled with a red arrowhead. At the bottom, methylation reaction was performed similarly except that 28*S* fragments were used at a concentration of 0.05 μM. Except noted, all primer extension was carried out with the *hyt* primer. An empty space indicates a component not added.

the full-length 28*S* rRNA (3970 nt), we synthesized several shorter derivatives that are progressively truncated at the 5′ end (Fig. 4, C and D): a 1990-nt fragment corresponding to a spontaneously generated 28*S* sub-fragment (fig. S3A), and a 1219-nt and a 779-nt fragments all containing the U base of interest. Results from the in vitro methylation assay largely recapitulate those using the in vivo rRNA as the substrate (Fig. 4, C and D). We were encouraged by these initial positive results and synthesized two even shorter RNA fragments centering around the modified U base (a 149-nt and a 99-nt fragment). Unfortunately, neither of these two shorter fragments could be efficiently used as substrates for Ptch methylation (Fig. 4D). In summary, our results suggest that the primary RNA sequence in combination with RNA structural elements is determinants of substrate recognition by Ptch. Although we have not been able to determine the minimal requirements for substrate recognition, we succeeded in reconstituting the entire m^3U reaction with in vitro components paving the way for in depth enzymology studies of Ptch/SPOUT1 in the future.

DISCUSSION

More than 30 years have passed since the discovery that the 28*S* rRNA from human is N^3 modified at a single U base. The enzyme responsible for this modification remains unknown until now. Here, we identified Ptch/SPOUT1 as the responsible enzyme for the m^3U modification on 28*S* rRNAs from higher eukaryotes. This m^3U modification is situated at the heart of the PTC domain of the large ribosomal subunit. *Drosophila* cells without this modification experience reduce protein synthesis capacity that ultimately leads to the death of the organism. Human cells deficient for the homologous enzyme do not survive as shown by others.

An evolutionarily ancient modification at PTC

m^3U modification is a conserved RNA modification, appearing in all kingdoms of life. Bioinformatic analyses suggest that it is likely catalyzed by the SPOUT class of RNA methyltransferases (*37*, *38*). An m^3U methyltransferase likely represents one of three SPOUT-class enzymes that modify rRNA, present in the last universal common ancestor (the other two being methyltransferases for 2′-*O*-methylation and m^1G). The bacterial RsmE enzyme and Bmt5 and Bmt6 enzymes from yeast, which catalyze m^3U formation at other positions on rRNAs from their respective species, might be homologs of Ptch/SPOUT1 that evolved in their respective domains of life.

At the PTC center of the large ribosomal subunit, the sequence of "5′-GGG**U**U" within which the modification falls on the first U is universally conserved. The functional importance of this U residue has been extensively investigated in a myriad of mutational studies in bacteria [e.g., (*50*–*53*)]. Also of particular interest is the finding that 2′-*O*-methylation mis-targeted to this U base has physiological consequences in yeast (*7*). Results from our study and others before suggest that the unique m^3U modification is present in animals, missing in yeast and possibly plants. Although it is missing in bacteria, it appears to be present in Archaea. A single m^3U base has been identified in 23*S* rRNA of the hyperthermophile *Sulfolobus solfactaricus* although the modified residue was not identified precisely (*54*). A careful reevaluation of rRNA modifications in *Haloarcula marismortui* identified an m^3U at PTC being one of only eight chemically modified sites in its 23S rRNA (*55*). The ethyl methanesulfonate (EMS)–induced EL-2 mutant strain of *Halobacterium salinarium*, which gained resistance to the antibiotic sparsomycin, was shown to be specifically missing the U-carried modification at PTC (*56*). Unfortunately, neither the nature of the U-carried modification nor the responsible enzyme has been identified in EL-2. Nevertheless, an enzyme responsible for this m^3U modification has been speculated for *Haloferax volcannii* (*57*), and Ptch/SPOUT1-homologous proteins are clearly present in archaeal genomes. Therefore, m^3U-modified PTC carries an ancient function that might have been replaced or made dispensable in certain domains of life such as bacteria and yeast. The identification of the m^3U methyltransferase here would spur renewed interests in this ancient modification.

The function of the m^3U modification at PTC

Although the solution conformations of 3-methyluridine have been solved (*58*), there is a lack of studies on the effect of m^3U on RNA chemistry. In vivo studies of m^3U on bacterial and fungal rRNAs yielded limited functional insights likely due to the lack of a strong physiological consequence in the enzyme mutants. On the contrary, the loss of a single methyl group at PTC causes lethality to human cells and *Drosophila* adults as we have shown here. From our characterization of the *Drosophila* mutants lacking the m^3U-modified PTC, we surmise that m^3U is not important for the proper processing of pre-rRNA but that normal translational efficiency measured by OPP incorporation into nascent peptides relies on its presence. However, the loss of total translational proficiency seems small.

Our last proposition is consistent with results from the characterization of the Archaean EL-2 mutant (*57*). Ribosomes purified from the EL-2 mutant had a reduced efficiency in conducting translation from a polyU RNA template. This reduction can be compensated by increasing the concentration of Mg^{2+} in the reaction, as compared to the wild-type situation where ribosomes lose their translational efficiency in the presence of heightened Mg^{2+} concentrations. Furthermore, the level of mature 70*S* ribosomes, which is reduced in EL-2, can yet again be restored with increasing Mg^{2+}. The ribosome is an important store of intracellular Mg^{2+}, where it interacts within the complex with both RNA and proteins, and is important for the overall structure of the ribosome [e.g., (*59*–*61*)]. Therefore, the loss of m^3U at PTC might alter a specific detail of the structure of this ribosomal center. This conclusion is further supported by the Archaean study in which the EL-2 mutation also changes the chemical accessibility of the neighboring U base, another universally conserved base with demonstrated importance. The combination of facile genetics in archaeal models and the recently developed system for introducing rRNA variants in vivo (*62*) are anticipated to facilitate the molecular characterization of m^3U's effect on ribosomal structure and function in this system, with implications for all domains of life.

Although loss of Ptch/SPOUT1 causes lethality in *Drosophila* and human cells, a partial loss of function mutation allows the emergence of sterile female and semi-sterile male flies. This disproportional effect on gamete production resembles Minute mutants with defective ribosomal proteins. We propose that gametic development demands a higher ribosomal function. In particular, eggs contain a large deposition of proteins and RNAs from the mother consistent with oogenesis being the most severely affected developmental process in these mutants. However, in the case of

Ptch, other possibilities exist. For examples, differential expression of *ptch* between the soma and the germlines and/or additional function carried out by Ptch in the germline, even one unrelated to it being an RNA methyltransferase, are all potential causes for the disproportional effect on gametic development upon its loss.

Substrate recognition by Ptch

Another major contribution from our study is the demonstration that the Ptch enzyme is both necessary and sufficient for catalyzing the specific m^3U modification. In particular, we succeeded in reconstituting the methylation reaction with recombinant components. In contrast, only partially purified ribosomes can serve as substrates for the other m^3U methyltransferases from bacteria or yeast (*17*, *26*). Recombinant human enzyme is capable of using the *Drosophila* RNA as a substrate, indicating that the determinants for substrate recognition must be conserved.

Although in vitro–synthesized 28*S* rRNA fragments longer than 700 nt serve effectively as substrates for Ptch, much shorter RNA molecules have not produced positive results, suggesting that RNA sequence alone is not sufficient for substrate recognition. Whether secondary structure(s) constitutes an essential element for such recognition requires further investigation. Nevertheless, our results suggest that other modifications on rRNA play negligible roles if any in Ptch's substrate recognition.

Our study, by no means, rules out the possibility that rRNA is the only biological substrate of Ptch/SPOUT1. A deeper understanding on how Ptch recognizes its rRNA target combined with the isolation of an m^3U specific antibody would facilitate the comprehensive identification of Ptch's substrates. Neither can we rule out the possibility that there are more than one m^3U base on *Drosophila* rRNA as we have not conducted a comprehensive MS analysis on fly rRNA. However, such analyses have been conducted for human, frog, and archaeal rRNAs (*28*, *29*, *55*), in which a single m^3U at PTC was identified in all cases. Therefore, it is likely the case also in flies.

Ptch as a potential target for "cancer antibiotics"

Most of the naturally occurring antibiotics target the ribosome. PTC is, by far, the most targeted region (*31*), suggesting that PTC is a naturally selected target for growth inhibition. Our study thus identified an important regulatory detail of ribosomal function in that the presence or absence of a single methyl group dictates cell survival in complex organisms.

This final conclusion leads us to propose that our results might lead to a new target for cancer therapy. A structural and chemical analysis of a large number of human RNA methyltransferases led to the suggestion that SPOUT1 is one of the most "druggable" enzymes, due to its cofactor binding pocket with the least charges and the highest extent of enclosure (*63*). Proliferation of cancer cells demands heightened ribosomal functions, and the nucleolus has been championed as an emerging target for cancer therapy (*64*). We speculate that a specific level of partial SPOUT1 inhibition could be achieved by small molecules so that growth of cancer cells is selectively inhibited. This aforementioned level of inhibition, disruptive to cancer but permissive to normal cellular growth, might be more achievable when the enzyme is easily druggable so that highly specific inhibitors are more likely to be recovered.

MATERIALS AND METHODS

Fly stocks, yeast strains, and animal cells

The following stocks were obtained from the Bloomington Drosophila Stock Center at Indiana, USA: BL#52669 has a *vasa*-driven *cas9* transgene producing Cas9 protein in the germlines, and BL#9539 [*Df(2R)BSC152/CyO*] carries a chromosomal deficiency of the *ptch* region. The w^{1118} stock was used as wild type. The construction of *ptch*-mutant lines and transgenic lines carrying *ptch* rescuing constructs is described below and illustrated in Fig. 1A. *Drosophila* stocks and crosses were maintained on a standard cornmeal medium and kept at 25°C.

The following samples were used for m^3U detection in rRNA from other species: SK1 strain of *Saccharomyces cerevisiae*, h90 strain of *Schizosaccharomyces pombe*, whole blood from mouse C57BL/6 strain, and cultured HeLa human cells.

CRISPR-Cas9–mediated mutagenesis of *ptch*

Cas9-induced *ptch* mutations were obtained using a transgenic approach in which Cas9 and sgRNA were expressed from two transgenes carrying either the *vasa* promoter for Cas9 expression or the *U6* promoter for sgRNA expression. sgRNA#1 with the sequence of 5′-ATTGCTTTAGCGGCTCTCC**AGG** (PAM sequence in bold) was used to generate frameshift mutations of $ptch^{7\text{-}7}$ [an insertion of 8 base pairs (bp) accompanied by a deletion of 4 bp, potentially encoding a truncated Ptch missing the last 116 residues] and $ptch^{12\text{–}2}$ (a 2-bp deletion, potentially encoding a C-terminally truncated Ptch protein). sgRNA#1 together with sgRNA#2, with the sequence of 5′-GGGAACAGCTATGCTCAGCG**TGG** (PAM in bold), was used to generate the deletion mutation of $ptch^{1\text{-}3}$ (a 955-bp deletion). All mutations were verified by PCR amplification followed by sequencing using DNA from homozygous animals as templates. PCR primers used for mutation detection are listed in table S1.

Construction of rescuing transgenic lines of *ptch*

A 5.8-kb DNA fragment from the genomic region of *ptch* (nucleotides 10025839 to 10031659 of chromosome *2R* in release dm6) that contains the endogenous regulatory elements of *ptch* was cloned into the vector of pUASTattB. Starting from this rescuing construct, we generated the $ptch^{G318AG322A}$ active site mutation by site-directed mutagenesis. Also starting from this construct, we inserted an *egfp* gene to the end of *ptch* before the STOP codon by bacterial recombineering, resulting in a transgene making GFP-tagged Ptch proteins. All transgenic constructs were inserted at 86F of chromosome *3R* by phiC31 integrase-mediated germline transformation and were subsequently introduced into a *ptch*-mutant background by genetic crossing. PCR primers for plasmid construction and verification are listed in table S1.

FISH and immunostaining

For FISH, salivary glands, ovaries, and testes of $ptch^{gfp}$ flies (full genotype: $ptch^{1\text{-}3}/^{1\text{-}3}$; $[ptch^{gfp}]/[ptch^{gfp}]$) were dissected in phosphate-buffered saline (PBS). Tissues were fixed in 4% paraformaldehyde for 4 hours. After being washed three times with 2× SSCT (0.1% Triton X-100), they were dehydrated using an ethanol gradient. After air drying, pre-hybridization was performed in 25% formamide, 5× Denhardt, 5% dextran sulfate, 2× SSC, 0.2% bovine serum albumin, and 125 μg of tRNA for 2 hours at 37°C. Tissues were incubated at 37°C overnight with a final probe concentration of 0.5 ng/ml. Post-hybridization washes were performed three times in 0.2×

SSCT for 15 min each. Tissues were then stained with DAPI (0.2 μg/ml in 4× SSCT) for 5 min, washed briefly in 4× SSCT, and allowed to air dry. Fluorescent images were captured by an Olympus IX83 confocal microscope. Probes are listed in table S1.

For immunostaining, salivary glands, ovaries, and testes of w^{1118} and $ptch^{gfp}$ were dissected in cold PBS. Tissues were fixed with a mixture of 3.7% formaldehyde diluted in PBS for 15 min. Heptane was subsequently added as a treatment for 30 min at room temperature. After the tissues were washed three times with 1× PBST (0.1% Triton X-100), they were incubated with a mouse anti-Fib antibody (from Abcam) overnight at 4°C. After another round of three washes with 1× PBST (0.1% Triton X-100), secondary antibody incubation was performed with Alexa Fluor 555–conjugated goat anti-mouse immunoglobulin G (1:200, Abcam), and DAPI was incubated for 1 hour. Fluorescent images (GFP fluorescence and anti-Fib signals) were photographed by an Olympus IX83 confocal microscope.

Analysis of rRNA by Northern blotting and qPCR

Northern hybridization analysis of 18*S* and 28*S* rRNAs was performed according to a protocol modified from (*17*). Total RNA was prepared by TRIzol reagent (Invitrogen, Carlsbad, California CA, USA). Total RNA (10 μg) each from adults of w^{1118}, $ptch^{7-7/12-2}$, and $ptch^{7-7/12-2}$; $[ptch^{+}]$ were separated on a 1% agarose gel in 1× tris-acetate-EDTA supplemented with 6.66% formaldehyde and transferred to a positively charged nylon membrane (Hybond N+, GE Healthcare) using capillary transfer. Northern hybridization analysis of 5.8*S* and 5*S* rRNAs was performed according to a protocol modified from (*65*). Agarose (1 g) was dissolved in 72 ml of water and cooled to 60°C in a water bath, followed by the addition of 10 mL of 10× Mops running buffer and 18 ml of 12.3 M formaldehyde. Total RNA (10 μg) from adults were dissolved in 11 μl of water and mixed with 5 μl of 10× Mops running buffer, 9 μl of 12.3 M formaldehyde, 25 μl of formamide, and 10 μl of formaldehyde loading buffer. The mixture was briefly centrifuged to collect the liquid and incubated for 15 min at 55°C. After electrophoresis, the gel was placed in a ribonuclease (RNase)–free glass dish and soaked for 45 min in 10 gel volumes of 20× SSC buffer. The RNA was transferred from the gel to a nylon membrane overnight. The membrane was rinsed in 2× SSC and allowed to dry, followed by immobilization of RNA with an ultraviolet transilluminator. The membrane was incubated with biotin-labeled DNA probes for 3 hours at 42°C with rotation, washed three times with 2× SSC at room temperature, after which 0.1% of SDS was added. A chemiluminescent biotin-labeled nucleic acid detection kit (Beyotime, China) was used to detect the signal using a manufacture provided protocol. Probe sequences were listed in table S1.

Total RNA from five female adults of w^{1118}, $ptch^{7-7/12-2}$, and $ptch^{7-7/12-2}$; $[ptch^{+}]$ were extracted using TRIzol reagent. cDNA was generated from 1 μg of total RNA using the PrimeScriptTM RT reagent kit (TaKaRa, Shiga, Japan) for the quantitation of rRNA by real-time qPCR. A Bio-Rad CFX96 Real-Time System (Bio-Rad, Hercules, CA, USA) and a KAPA SYBR FAST Universal qPCR Kit (Kapa Biosystems, Boston, MA, USA) were used. The cDNA standard for each gene was diluted to different concentrations and used as template for PCR reactions. The expression of *rp49* was used as a control. The standard curves of these genes were drawn with the logarithm of the copy number of template DNA as the abscissa and the measured CT value as the ordinate. The initial copy number of 18*S* rRNA, 28*S* rRNA, 5.8*S* rRNA, or 5*S* rRNA was calculated from the CT value of each cDNA sample after adjustment with *rp49*. Each quantification was done in three biological replicates. The primers are listed in table S1.

Primer extension for the detection of m^3U

Two 5′ biotin-labeled DNA primers (HYT and 2R) were used for primer extension. A primer/RNA pre-mixture containing 8 μl of RNase-free water, 1 μl of primer (1 pmol), and 1 μg of template RNA per reaction was denatured at 70°C for 3 min and then chilled on ice. After incubation at 42°C for 10 min, 5× M-MLV reverse transcription buffer, dNTP mix (final concentration of 1 mM), 200 U of M-MLV reverse transcriptase (Promega), and RNase-free water were added to make up a 25-μl reaction. The primer extension reaction was performed at 42°C for 1 hour, and DNA products were separated on 40% polyacrylamide–8 M urea gels. To generate markers for the primer extension products, a DNA sequencing reaction was performed by a standard protocol. Briefly, the 28*S* ribosomal DNA of *Drosophila melanogaster* was PCR amplified and cloned into the pMD-18 T vector. A 15-μl sequencing reaction mixture was assembled from 1 μg of the above plasmid, 10 U of Taq DNA polymerase (Promega), 5 μl of a ddNTP mixture, 3 μl of 5× Taq buffer, and 1 pmol of the biotin-labeled primer. The content of the sequencing reaction was run along with the primer extension products, transferred to nylon membranes, and developed using streptavidin–horseradish peroxidase.

Small rRNA fragment purification by mung bean nuclease protection

A mung bean nuclease protection assay was modified from a protocol described in (*42*). Briefly, a 175 μl of DNA/RNA mixture, containing 10 μl of the protecting DNA oligonucleotides (oligos) and 100 μg of total *Drosophila* RNA, was incubated with 10% dimethyl sulfoxide (DMSO) in 0.3 volume of hybridization buffer (250mM Hepes, 500 mM KCl, and 5% DMSO at pH 7) at 90°C for 5 min and then slowly cooled to room temperature over 2 hours. After this hybridization step, 20 μl of 10× mung bean nuclease buffer [New England Biolabs (NEB)] and 4 μl of the nuclease (NEB) along with 1 μl of RNase A (Sigma-Aldrich) were added to the digestion and allowed to react for 1 hour at 35°C. After the digestion step, the protected fragment (DNA-RNA hybrid) was extracted by phenol/chloroform extraction, followed by ethanol precipitation overnight. The protected rRNA fragments were separated from the complementary DNA oligos on a denaturing 13% polyacrylamide–8 M urea gel and were excised and eluted in elution buffer [1 mM ethylenediaminetetraacetic acid, 0.1% SDS, and 0.4 M NaOAc (pH 5.2)] at 25°C for 4 hours. Three volumes of ethanol were added to precipitate RNA fragments. For producing the LC-MS/MS samples in Fig. 2G, the 34-nt "m^3U protecting" oligo was used that has the sequence of 5′-**A**CCCAGCT ACGTTCCCTTGCATGGGTGAACAAT-3′, in which the A pairing with the m^3U base is labeled here in bold. For the "no protection" sample, the 30-nt oligo was used that has the sequence of 5′-AGCTA CGTTCCCTTGCATGGGTGAACAAT-3′.

RTL-P and RP-HPLC analyses of m^3U

RTL-P was prepared as described in (*41*). The specific RT primer and two forward primers for PCR amplification are listed in table S1.

For reversed-phase HPLC (RP-HPLC) analysis of m^3U modifications, the protected RNA fragments from the mung bean nuclease protection assay were denatured for 2 min, followed by rapid

cooling on ice. After digestion to completion by nuclease P1 and alkaline phosphatase, the hydrolysate was analyzed by HPLC according to the method described in (*42*). Briefly, nucleosides were loaded on a Supelcosil LC-18-S HPLC column (25 cm by 4.6 mm, 5 μm) at 25°C on a Dionex UltiMate 3000 HPLC system (Thermo Fisher Scientific). For m^3U detection, the 254 nm of absorption peak wavelength was used. The elution conditions for m^3U were changed to a gradient mode using 100% buffer A [10 mM of $NH_4H_2PO_4$ and 2.5% of methanol (pH 5.3)] for 20 min, 90% buffer and 10% buffer B [10 mM of $NH_4H_2PO_4$ and 20% of methanol (pH 5.1)] for 5 min, 75% buffer A and 25% buffer B for 11 min, 50% buffer A and 50% buffer B for 9 min, and 100% buffer B for 20 min. Buffer C [10 mM of $NH_4H_2PO_4$ and 35% of acetonitrile (pH 4.9)] was used to clean and recycle the column after each run. The flow rate was 1 ml/min.

UHPLC-MS/MS analysis of m^3U

The level of m^3U was determined by Wuhan Greensword Creation Technology Co. Ltd., China (www.greenswordcreation.com) based on ultrahigh-performance liquid chromatography (UHPLC)–MS/MS analysis (Thermo Scientific Ultimate 3000 UHPLC coupled with TSQ Quantiva). In brief, the isolated RNA was enzymatically digested according to previously described method (*66*). The chromatographic separation was performed on a Shimadzu Shim-pack C18 column (100 mm by 2.1 mm, inside diameter of 2.0 μm) at 40°C with 0.05% formic acid aqueous solution (solvent A) and methanol (solvent B) as the mobile phases. The mass spectrometry detection was performed under positive electrospray ionization mode. The target nucleosides were monitored by multiple reaction monitoring mode using the mass transitions (precursor ions to product ions) of m^3U (259.1 to 127.1) and of rU (245.1 to 113.0). The LOD and LOQ for the procedure were 0.93 and 3.09 fmol, respectively. Triplicate samples were analyzed.

Knockdown of human SPOUT1 by RNAi

siRNAs were obtained from RIBBIO (Guangzhou, China). HeLa cells were plated on 24-well plates and grown to 50% confluence. Cells were transfected using Lipofectamine RNAiMAX (Invitrogen) with 100 nM NC siRNA or SPOUT1 siRNAs (si-1, GCAGGACCCUCGCACCAAA; si-2, GCACCAGGAUCUACAGUUU; and si-3, GUGUCCUCUUUGACCUGUA). After 48, 72, and 96 hours of growth, cells were lysed with TRIzol. Total RNA was reverse transcribed to detect the expression level of *SPOUT1* with *gapdh* used as a control. In addition, total RNA was reverse transcribed with specific primers for the detection of m^3U by RTL-P. Three biological replicates were included. The primers are listed in table S1.

Op-puro labeling of cells and protein detection by fluorescence

Labeling was performed with Click-iT Plus OPP Protein Synthesis Assay Kits (Thermo Fisher Scientific, C10456) and Click-iT Protein Reaction Buffer Kit (Thermo Fisher Scientific, C10276) on tissues. Tissues (brain, disc, and salivary glands of larvae, testes, and ovaries of adult flies) were dissected in Schneider's medium, transferred to Schneider's medium with 20 μM OPP, and incubated for 0.5 or 2 hours. Samples were washed with PBS briefly and then homogenized in lysis buffer (1% SDS, 50 mM tris-HCl, 1 mM $MgCl_2$, 1 μl of Benzonase, and protease inhibitor cocktail). After 5 min of lysis, a click reaction was performed per the protocol from kit (Thermo Fisher Scientific, C10276) for 30 min, with continuous vortexing. Following centrifugation for 3 min, the supernatant was transferred to a new tube with Laemmli buffer and heated for 10 min at 98°C. Protein samples prepared as above were subjected to SDS–polyacrylamide gel electrophoresis. The gel was fixed with a solution of 60% methanol and 30% acetic acid, detected for Alexa-488 and subsequently stained with Coomassie blue for total protein quantification. Experiments on different genotypes were performed in at least three biological replicates. Different durations of OPP incubation (0.5 or 2 hours) yield similar conclusions.

Expression and purification of Ptch recombinant proteins

The open reading frame sequences of Ptch and SPOUT1 were cloned into the expression vector pLOU3 (*67*), in which the target protein is tagged at its N terminus with a His6 tag followed by an MPB tag. Site-directed mutagenesis was used to introduce the $ptch^{G318AG322A}$ active site mutation into the above pLOU3-Ptch vector. The expression plasmids were transformed into *E. coli* BL21(DE3) for isopropyl-β-D-thiogalactopyranoside (0.5 mM)–induced protein expression. Soluble proteins were purified by a standard Ni–nitrilotriacetic acid resin–based method and eluted with imidazole. Eluted proteins were buffer exchanged against PBS with 600 mM trehalose and 30% glycerol at room temperature through PD SpinTrap G-25 columns (Cytiva) and frozen in small aliquots and stored at −80°C.

In vitro m^3U methylation assay

Total RNA (800 μg) from $ptch^{7-7/7-7}$ adults was reconstituted in 1× methylation buffer [50 mM tris-HCl, 50 mM NaCl, 10 mM $MgCl_2$, 10 mM dithiothreitol, and 0.5 U of RNase Inhibitor (pH 8.0)] at room temperature for 5 min. Various amounts of recombinant MBP-Ptch proteins (see legends of Fig. 4) were added to the RNA mixture with a final volume of 20 μl, followed by the addition of 5 μl of SAM in a final concentration of 0.5 mM. After incubation at 25°C for 1 hour, RNA was purified from the methylation mixture by phenol/chloroform extraction, followed by ethanol precipitation overnight. Purified RNA was subject to m^3U detection by primer extension as described above.

To synthesize RNA substrates for the methylation assay, fragments of 28*S* rDNA were amplified by PCR using forward primers containing promoter sequence for the T7 RNA polymerase (table S1). 28*S* rRNA fragments were synthesized using a T7 RiboMAXTM Express Large Scale RNA Production System (Promega, Wisconsin, Madison, USA) following the manufacturer's instruction. Synthesized RNA was purified by phenol/chloroform extraction followed by ethanol precipitation and, subsequently, used for in vitro methylation as described above.

The reaction specifics for Fig. 4A are as follows. For each methylation reaction, 800 ng ("+" lanes), 1.6 μg ("++" lanes), or 2.4 μg ("+++" lanes) of total RNA were used. MBP-Ptch concentrations were 0.5, 1.0, and 4.0 μM (for the gradient) and 4.0 μM (for + lanes). The $MBP\text{-}Ptch^{am}$ concentrations were 2.0, 4.0, and 12 μM (for the gradient) and 12 μM (for + lanes). The SAM cofactor was used at 1.0 mM (+ lanes). Reaction specifics for Fig. 4B are as follows. In vitro methylation reaction was performed similarly to the one shown Fig. 4A except for the following ingredients. MBP-Ptch concentrations were 30, 60, and 120 μM (for the gradient) and 120 μM (for + lanes). The $MBP\text{-}Ptch^{am}$ concentrations were 0.1, 0.2, and 0.6 mM (for the gradient) and 0.6 mM (for + lanes). A recombinant human MBP-SPOUT1 enzyme was used at a concentration of 30, 60, and 120 μM (for the

gradient) and 120 μM (for + lanes). SAM was used at 0.5 mM (+ lanes). Reaction specifics for Fig. 4C are as follows. In vitro methylation reaction was performed similarly to the one shown in Fig. 4 (A and B) except for the following ingredients. A reaction was included with the full-length 28*S* rRNA transcribed in vitro (*28Sab*; see Fig. 4D for details) used as the RNA substrate at the following concentrations: 0.05 μM (+ lanes), 0.15 μM (++ lanes), and 0.25 μM (+++ lanes).

Statistical analyses

All data are summarized as the means ± SE. One-way analysis of variance (ANOVA; Fisher's least significant difference) was used to analyze the differences between four groups for multiple comparisons (fig. S1B). A two-tailed unpaired Student's *t* test was used to analyze the differences between two groups in Figs. 1C and 2G and figs. S2C and S3C. Analyses were conducted using the SPSS software (version 20.0; IBM Corp., Armonk, NY, USA).

Supplementary Materials

This PDF file includes:

Figs. S1 to S4
Table S1

REFERENCES AND NOTES

1. K. E. Sloan, A. S. Warda, S. Sharma, K.-D. Entian, D. L. J. Lafontaine, M. T. Bohnsack, Tuning the ribosome: The influence of rRNA modification on eukaryotic ribosome biogenesis and function. *RNA Biol.* **14**, 1138–1152 (2017).
2. P. V. Sergiev, N. A. Aleksashin, A. A. Chugunova, Y. S. Polikanov, O. A. Dontsova, Structural and evolutionary insights into ribosomal RNA methylation. *Nat. Chem. Biol.* **14**, 226–235 (2018).
3. P. Londei, S. Ferreira-Cerca, Ribosome biogenesis in archaea. *Front. Microbiol.* **12**, 686977 (2021).
4. D. Streit, E. Schleiff, The Arabidopsis 2′-O-ribose-methylation and pseudouridylation landscape of rRNA in comparison to human and yeast. *Front. Plant Sci.* **12**, 684626 (2021).
5. M. Helm, Post-transcriptional nucleotide modification and alternative folding of RNA. *Nucleic Acids Res.* **34**, 721–733 (2006).
6. J. L. Baxter-Roshek, A. N. Petrov, J. D. Dinman, Optimization of ribosome structure and function by rRNA base modification. *PLOS ONE* **2**, e174 (2007).
7. B. Liu, X. H. Liang, D. Piekna-Przybylska, Q. Liu, M. J. Fournier, Mis-targeted methylation in rRNA can severely impair ribosome synthesis and activity. *RNA Biol.* **5**, 249–254 (2008).
8. A. Baudin-Baillieu, C. Fabret, X.-H. Liang, D. Piekna-Przybylska, M. J. Fournier, J. P. Rousset, Nucleotide modifications in three functionally important regions of the *Saccharomyces cerevisiae* ribosome affect translation accuracy. *Nucleic Acids Res.* **37**, 7665–7677 (2009).
9. S. K. Mahto, C. S. Chow, Probing the stabilizing effects of modified nucleotides in the bacterial decoding region of 16S ribosomal RNA. *Bioorg. Med. Chem.* **21**, 2720–2726 (2013).
10. J. Erales, V. Marchand, B. Panthu, S. Gillot, S. Belin, S. E. Ghayad, M. Garcia, F. Laforêts, V. Marcel, A. Baudin-Baillieu, P. Bertin, Y. Couté, A. Adrait, M. Meyer, G. Therizols, M. Yusupov, O. Namy, T. Ohlmann, Y. Motorin, F. Catez, J. J. Diaz, Evidence for rRNA 2′-O-methylation plasticity: Control of intrinsic translational capabilities of human ribosomes. *Proc. Natl. Acad. Sci. U.S.A.* **114**, 12934–12939 (2017).
11. E. S. Maxwell, M. J. Fournier, The small nucleolar RNAs. *Annu. Rev. Biochem.* **64**, 897–934 (1995).
12. Z. Kiss-László, Y. Henry, J. P. Bachellerie, M. Caizergues-Ferrer, T. Kiss, Site-specific ribose methylation of preribosomal RNA: A novel function for small nucleolar RNAs. *Cell* **85**, 1077–1088 (1996).
13. E. K. Borchardt, N. M. Martinez, W. V. Gilbert, Regulation and function of RNA pseudouridylation in human cells. *Annu. Rev. Genet.* **54**, 309–336 (2020).
14. K. Sirum-Connolly, T. L. Mason, Functional requirement of a site-specific ribose methylation in ribosomal RNA. *Science* **262**, 1886–1889 (1993).
15. C. Bonnerot, L. Pintard, G. Lutfalla, Functional redundancy of Spb1p and a snR52-dependent mechanism for the 2′-O-ribose methylation of a conserved rRNA position in yeast. *Mol. Cell* **12**, 1309–1315 (2003).
16. B. Lapeyre, S. K. Purushothaman, Spb1p-directed formation of Gm2922 in the ribosome catalytic center occurs at a late processing stage. *Mol. Cell* **16**, 663–669 (2004).
17. S. Sharma, J. Yang, S. Düttmann, P. Watzinger, P. Kötter, K.-D. Entian, Identification of novel methyltransferases, Bmt5 and Bmt6, responsible for the m3U methylations of 25S rRNA in *Saccharomyces cerevisiae*. *Nucleic Acids Res.* **42**, 3246–3260 (2014).
18. G. Bourgeois, M. Ney, I. Gaspar, C. Aigueperse, M. Schaefer, S. Kellner, M. Helm, Y. Motorin, Eukaryotic rRNA modification by yeast 5-methylcytosine-methyltransferases and human proliferation-associated antigen p120. *PLOS ONE* **10**, e0133321 (2015).
19. C. P. J. J. van Buul, W. Visser, P. H. van Knippenberg, Increased translational fidelity caused by the antibiotic kasugamycin and ribosomal ambiguity in mutants harbouring the *ksgA* gene. *FEBS Lett.* **177**, 119–124 (1984).
20. P. Pletnev, E. Guseva, A. Zanina, S. Evfratov, M. Dzama, V. Treshin, A. Pogorel'skaya, I. Osterman, A. Golovina, M. Rubtsova, M. Serebryakova, O. V. Pobeguts, V. M. Govorun, A. A. Bogdanov, O. A. Dontsova, P. V. Sergiev, Comprehensive functional analysis of *Escherichia coli* ribosomal RNA methyltransferases. *Front. Genet.* **11**, 97 (2020).
21. H. Ma, X. Wang, J. Cai, Q. Dai, S. K. Natchiar, R. Lv, K. Chen, Z. Lu, H. Chen, Y. G. Shi, F. Lan, J. Fan, B. P. Klaholz, T. Pan, Y. Shi, C. He, N^6 methyladenosine methyltransferase ZCCHC4 mediates ribosomal RNA methylation. *Nat. Chem. Biol.* **15**, 88–94 (2019).
22. N. van Tran, F. G. M. Ernst, B. R. Hawley, C. Zorbas, N. Ulryck, P. Hackert, K. E. Bohnsack, M. T. Bohnsack, S. R. Jaffrey, M. Graille, D. L. J. Lafontaine, The human 18S rRNA m6A methyltransferase METTL5 is stabilized by TRMT112. *Nucleic Acids Res.* **47**, 7719–7733 (2019).
23. R. Pinto, C. B. Vågbø, M. E. Jakobsson, Y. Kim, M. P. Baltissen, M.-F. O'Donohue, U. H. Guzmán, J. M. Małecki, J. Wu, F. Kirpekar, J. V. Olsen, P. E. Gleizes, M. Vermeulen, S. A. Leidel, G. Slupphaug, P. Ø. Falnes, The human methyltransferase ZCCHC4 catalyses N^6-methyladenosine modification of 28S ribosomal RNA. *Nucleic Acids Res.* **48**, 830–846 (2020).
24. C. Sepich-Poore, Z. Zheng, E. Schmitt, K. Wen, Z. S. Zhang, X.-L. Cui, Q. Dai, A. C. Zhu, L. Zhang, A. Sanchez Castillo, H. Tan, J. Peng, X. Zhuang, C. He, S. Nachtergaele, The $METTL_5$-TRMT112 N^6-methyladenosine methyltransferase complex regulates mRNA translation *via* 18S rRNA methylation. *J. Biol. Chem.* **298**, 101590 (2022).
25. G. N. Basturea, K. E. Rudd, M. P. Deutscher, Identification and characterization of RsmE, the founding member of a new RNA base methyltransferase family. *RNA* **12**, 426–434 (2006).
26. G. N. Basturea, M. P. Deutscher, Substrate specificity and properties of the *Escherichia coli* 16S rRNA methyltransferase, RsmE. *RNA* **13**, 1969–1976 (2007).
27. H. Zhang, H. Wan, Z. Q. Gao, Y. Wei, W. J. Wang, G. F. Liu, E. V. Shtykova, J. H. Xu, Y. H. Dong, Insights into the catalytic mechanism of 16S rRNA methyltransferase RsmE (m^3U1498) from crystal and solution structures. *J. Mol. Biol.* **423**, 576–589 (2012).
28. B. E. Maden, The numerous modified nucleotides in eukaryotic ribosomal RNA. *Prog. Nucleic Acid Res. Mol. Biol.* **39**, 241–303 (1990).
29. M. Taoka, Y. Nobe, Y. Yamaki, K. Sato, H. Ishikawa, K. Izumikawa, Y. Yamauchi, K. Hirota, H. Nakayama, N. Takahashi, T. Isobe, Landscape of the complete RNA chemical modifications in the human 80S ribosome. *Nucleic Acids Res.* **46**, 9289–9298 (2018).
30. D. Piekna-Przybylska, W. A. Decatur, M. J. Fournier, The 3D rRNA modification maps database: With interactive tools for ribosome analysis. *Nucleic Acids Res.* **36**, D178–D183 (2008).
31. N. Polacek, A. S. Mankin, The ribosomal peptidyl transferase center: Structure, function, evolution, inhibition. *Crit. Rev. Biochem. Mol. Biol.* **40**, 285–311 (2005).
32. Q. Peng, Y. Wang, Y. Xiao, H. Chang, S. Luo, D. Wang, Y. S. Rong, *Drosophila* Amus and Bin3 methylases functionally replace mammalian MePCE for capping and the stabilization of U6 and 7SK snRNAs. *Sci. Adv.* **9**, eadj9359 (2023).
33. S. Saebøe-Larssen, M. Lyamouri, J. Merriam, M. P. Oksvold, A. Lambertsson, Ribosomal protein insufficiency and the minute syndrome in Drosophila: A dose-response relationship. *Genetics* **148**, 1215–1224 (1998).
34. S. J. Marygold, J. Roote, G. Reuter, A. Lambertsson, M. Ashburner, G. H. Millburn, P. M. Harrison, Z. Yu, N. Kenmochi, T. C. Kaufman, S. J. Leevers, K. R. Cook, The ribosomal protein genes and *Minute* loci of *Drosophila melanogaster*. *Genome Biol.* **8**, R216 (2007).
35. T. Wang, K. Birsoy, N. W. Hughes, K. M. Krupczak, Y. Post, J. J. Wei, E. S. Lander, D. M. Sabatini, Identification and characterization of essential genes in the human genome. *Science* **350**, 1096–1101 (2015).
36. T. Treiber, N. Treiber, U. Plessmann, S. Harlander, J. L. Daiß, N. Eichner, G. Lehmann, K. Schall, H. Urlaub, G. Meister, A compendium of RNA-binding proteins that regulate MicroRNA biogenesis. *Mol. Cell* **66**, 270–284.e13 (2017).
37. V. Anantharaman, E. V. Koonin, L. Aravind, SPOUT: A class of methyltransferases that includes spoU and trmD RNA methylase superfamilies, and novel superfamilies of predicted prokaryotic RNA methylases. *J. Mol. Microbiol. Biotechnol.* **4**, 71–75 (2002).
38. K. L. Tkaczuk, S. Dunin-Horkawicz, E. Purta, J. M. Bujnicki, Structural and evolutionary bioinformatics of the SPOUT superfamily of methyltransferases. *BMC Bioinformatics* **8**, 73 (2007).
39. H. Hori, Transfer RNA methyltransferases with a SpoU-TrmD (SPOUT) fold and their modified nucleosides in tRNA. *Biomolecules* **7**, 23 (2017).

40. S. E. Strassler, I. E. Bowles, D. Dey, J. E. Jackman, G. L. Conn, Tied up in knots: Untangling substrate recognition by the SPOUT methyltransferases. *J. Biol. Chem.* **298**, 102393 (2022).
41. Z. W. Dong, P. Shao, L. T. Diao, H. Zhou, C. H. Yu, L. H. Qu, RTL-P: A sensitive approach for detecting sites of 2′-O-methylation in RNA molecules. *Nucleic Acids Res.* **40**, e157 (2012).
42. J. Yang, S. Sharma, P. Watzinger, J. D. Hartmann, P. Kötter, K. D. Entian, Mapping of complete set of ribose and base modifications of yeast rRNA by RP-HPLC and mung bean nuclease assay. *PLOS ONE* **11**, e0168873 (2016).
43. J. Liu, Y. Xu, D. Stoleru, A. Salic, Imaging protein synthesis in cells and tissues with an alkyne analog of puromycin. *Proc. Natl. Acad. Sci. U.S.A.* **109**, 413–418 (2012).
44. C. H. Lee, M. Kiparaki, J. Blanco, V. Folgado, Z. Ji, A. Kumar, G. Rimesso, N. E. Baker, A regulatory response to ribosomal protein mutations controls translation, growth, and cell competition. *Dev. Cell* **46**, 456–469.e4 (2018).
45. H. Y. Chan, S. Brogna, C. J. O'Kane, Dribble, the *Drosophila* KRR1p homologue, is involved in rRNA processing. *Mol. Biol. Cell* **12**, 1409–1419 (2001).
46. K. E. Bohnsack, M. T. Bohnsack, Uncovering the assembly pathway of human ribosomes and its emerging links to disease. *EMBO J.* **38**, e100278 (2019).
47. G. Michel, V. Sauvé, R. Larocque, Y. Li, A. Matte, M. Cygler, The structure of the RlmB 23S rRNA methyltransferase reveals a new methyltransferase fold with a unique knot. *Structure* **10**, 1303–1315 (2002).
48. A. B. Taylor, B. Meyer, B. Z. Leal, P. Kötter, V. Schirf, B. Demeler, P. J. Hart, K.-D. Entian, J. Wöhnert, The crystal structure of Nep1 reveals an extended SPOUT-class methyltransferase fold and a pre-organized SAM-binding site. *Nucleic Acids Res.* **36**, 1542–1554 (2008).
49. A. Hernández-Cid, J. Lozano-Aponte, T. Scior, Molecular dynamics and docking simulations of homologous RsmE methyltransferases hints at a general mechanism for substrate release upon uridine methylation on 16S rRNA. *Int. J. Mol. Sci.* **24**, 16722 (2023).
50. B. T. Porse, H. P. Thi-Ngoc, R. A. Garrett, The donor substrate site within the peptidyl transferase loop of 23 S rRNA and its putative interactions with the CCA-end of N-blocked aminoacyl-tRNA^{Phe}. *J. Mol. Biol.* **264**, 472–483 (1996).
51. R. Green, H. F. Noller, Reconstitution of functional 50S ribosomes from in vitro transcripts of *Bacillus stearothermophilus* 23S rRNA. *Biochemistry* **38**, 1772–1779 (1999).
52. E. M. Youngman, J. L. Brunelle, A. B. Kochaniak, R. Green, The active site of the ribosome is composed of two layers of conserved nucleotides with distinct roles in peptide bond formation and peptide release. *Cell* **117**, 589–599 (2004).
53. A. E. d'Aquino, T. Azim, N. A. Aleksashin, A. J. Hockenberry, A. Krüger, M. C. Jewett, Mutational characterization and mapping of the 70S ribosome active site. *Nucleic Acids Res.* **48**, 2777–2789 (2020).
54. K. R. Noon, E. Bruenger, J. A. McCloskey, Posttranscriptional modifications in 16S and 23S rRNAs of the archaeal hyperthermophile *Sulfolobus solfataricus*. *J. Bacteriol.* **180**, 2883–2888 (1998).
55. F. Kirpekar, L. H. Hansen, A. Rasmussen, J. Poehlsgaard, B. Vester, The archaeon *Haloarcula marismortui* has few modifications in the central parts of its 23S ribosomal RNA. *J. Mol. Biol.* **348**, 563–573 (2005).
56. E. Lázaro, C. Rodriguez-Fonseca, B. Porse, D. Ureña, R. A. Garrett, J. P. Ballesta, A sparsomycin-resistant mutant of *Halobacterium salinarium* lacks a modification at nucleotide U2603 in the peptidyl transferase centre of 23 S rRNA. *J. Mol. Biol.* **261**, 231–238 (1996).
57. H. Grosjean, C. Gaspin, C. Marck, W. A. Decatur, V. de Crécy-Lagard, RNomics and Modomics in the halophilic archaea *Haloferax volcanii*: Identification of RNA modification genes. *BMC Genomics* **9**, 470 (2008).
58. J. P. Desaulniers, H. M. Chui, C. S. Chow, Solution conformations of two naturally occurring RNA nucleosides: 3-Methyluridine and 3-methylpseudouridine. *Bioorg. Med. Chem.* **13**, 6777–6781 (2005).
59. V. K. Misra, D. E. Draper, On the role of magnesium ions in RNA stability. *Biopolymers* **48**, 113–135 (1998).
60. A. S. Petrov, C. R. Bernier, C. Hsiao, C. D. Okafor, E. Tannenbaum, J. Stern, E. Gaucher, D. Schneider, N. V. Hud, S. C. Harvey, L. D. Williams, RNA-magnesium-protein interactions in large ribosomal subunit. *J. Phys. Chem. B* **116**, 8113–8120 (2012).
61. K. H. Nierhaus, Mg^{2+}, K^{+}, and the ribosome. *J. Bacteriol.* **196**, 3817–3819 (2014).
62. M. Jüttner, M. Weiß, N. Ostheimer, C. Reglin, M. Kern, R. Knüppel, S. Ferreira-Cerca, A versatile cis-acting element reporter system to study the function, maturation and stability of ribosomal RNA mutants in archaea. *Nucleic Acids Res.* **48**, 2073–2090 (2020).
63. M. Schapira, Structural chemistry of human RNA methyltransferases. *ACS Chem. Biol.* **11**, 575–582 (2016).
64. N. Hein, K. M. Hannan, A. J. George, E. Sanij, R. D. Hannan, The nucleolus: An emerging target for cancer therapy. *Trends Mol. Med.* **19**, 643–654 (2013).
65. T. Brown, K. Mackey, T. Du, Analysis of RNA by northern and slot blot hybridization. *Curr. Protoc. Mol.* **67**, 9 (2004).
66. F. Shen, W. Huang, J. T. Huang, J. Xiong, Y. Yang, K. Wu, G. F. Jia, J. Chen, Y. Q. Feng, B. F. Yuan, S. M. Liu, Decreased N^6-methyladenosine in peripheral blood RNA from diabetic patients is associated with FTO expression rather than ALKBH5. *J. Clin. Endocrinol. Metab.* **100**, E148–E154 (2015).
67. X. Qi, W. Wang, H. Dong, Y. Liang, C. Dong, H. Ly, Expression and X-ray structural determination of the nucleoprotein of Lassa fever virus. *Methods Mol. Biol.* **1604**, 179–188 (2018).

Acknowledgments: We thank X. Tan at the University of South China for technical assistance and N. Misunou at EMBL for critical comments on the manuscript. **Funding:** This work was supported by the National Natural Science Foundation of China, 3221101328 to Y.S.R., 32472563 to J.C., and 32300524 to Y.H.; a special fund for scientific innovation strategy-construction of high level Academy of Agricultural Sciences, R2023PY-JX010 to J.C.; the National Natural Science Foundation of Hunan Province China, 2023JJ40536 to M.C.; and a startup fund from the University of South China to Y.S.R. **Author contributions:** Conceptualization: J.C., Y.B., Y.H., M.C., and Y.S.R. Methodology: J.C., Y.B., Y.H., M.C., and Y.S.R. Investigation: J.C., Y.B., Y.H., M.C., Y.W., Z.G., X.W., Y.L., and Y.S.R. Visualization: J.C., Y.B., Y.H., M.C., and Y.S.R. Supervision: Y.S.R. Writing—original draft: J.C. and Y.S.R. Writing—review and editing: J.C., Y.B., Y.H., M.C., and Y.S.R. **Competing interests:** The authors declare that they have no competing interests. **Data and materials availability:** All data needed to evaluate the conclusions in the paper are present in the paper and/or the Supplementary Materials. *Drosophila* stocks, plasmids, and antibodies are freely available from Y.S.R.

Submitted 18 June 2024
Accepted 5 November 2024
Published 13 December 2024
10.1126/sciadv.adr1743